

Seismic attribute selection and clustering to detect and classify surface waves in multicomponent seismic data by using *k*-means algorithm

Ivan Sánchez Galvis¹, Yenni Villa¹, César Duarte¹, Daniel Sierra¹, and William Agudelo²

Abstract

Seismic records are characterized by a high level of complexity resulting from the interaction of different types of waves propagating in the subsurface. Interpretation of the different wave modes and features present in a seismic record generally is done by expert judgment, and its automatization is a problem that has not been resolved completely. We present a methodology that uses pattern recognition to select the best seismic attributes that should be chosen to detect and classify surface waves in a seismic record, based on the notion of similarity, and that is applied on the automatic interpretation of three different seismic-data record sets. The classification obtained for these different real data sets exhibits well-differentiated zones that improve and automatize the expert judgment interpretation.

Introduction

In the last decades, dozens of different seismic attributes have been proposed to detect, characterize, and filter surface waves (a partial list is presented in Table 1). It is difficult to decide which of these attributes are best applied on a particular case or even if they are independent or not. Pattern recognition provides a data-driven way to classify which attributes contribute the most to detect surface waves on a specific case. Surface-wave detection could be considered the first stage before its separation, which is possible by locally filtering through attributes that differentiate surface waves from other wave modes. When detection is not properly done, essential information about wave modes of interest (e.g., reflections) can be lost since filtering will remove different wave modes indiscriminately. The proper use of filters reduces the possible damage to the signal since they operate within the record intervals in which the surface waves are detected.

Fundamentally, surface waves differ from body waves in frequency content, polarization, dispersion, and propagation velocity. However, in real cases, surface waves can exhibit a very complex behavior: (1) because of near-surface heterogeneities, surface-wave scattering can be produced, and a great part of the energy may have an incidence out of the receiver-source plane; and (2) surface waves involve modes other than a pure Rayleigh wave produced when the medium is not homogeneous (Sheriff, 2002). Therefore, surface-wave classification generally is done by expert (human) judgment, and its automatization is a problem that has not been solved completely. A careful examination of a seismic record shows that there are different regions inside a surface-wave cone, each with its own seismic attributes characteristics.

Figure 1a displays a real 3C seismic exploration record, where the vertical, radial, and transverse components are given from left to right. There, the surface-wave cone is interpreted, by

human judgment, as the area under the dashed yellow curve. To illustrate the seismic attribute differences between surface and body waves, one seismic trace is extracted to compute the spectra and the hodogram of the data within a time sliding window. When this sliding window travels along the body-wave zone, the frequency content ranges from 30 to 50 Hz, and the polarization tends to be linear, as shown in the normalized spectra and hodogram of Figure 1b. In contrast, when the sliding window crosses the surface-wave area, in Figure 1c, the frequency content is much lower, ranging from 5 to 15 Hz, and polarization tends to be elliptical. These basic attribute differences can be used to separate surface waves from reflection waves. Hence, a primary classification by frequency content and polarization is evident. However, real cases show that this simple classification (based on frequency filtering or simple polarization attributes) is not adequate for complex surface waves. By using a more complete set of seismic attributes, it is possible to quantify the behavior of the wavefield propagation from seismic data. Then, one question arises: which and how many attributes are required to obtain an accurate classification for seismic waves?

This work was motivated by the results obtained in Sánchez et al. (2016) in which the goal was ground-roll attenuation by polarization filtering. In that work, only two attributes, namely ellipticity and planarity, were computed followed by the detection and classification of surface waves by human judgment. The aim of this paper is to show that it is possible to perform this detection and classification automatically using pattern-recognition techniques that allow us to separate the information with different behavior using an arbitrary number of attributes.

Pattern-recognition tools allow us to minimize errors in the classification process. These tools have been applied widely in seismic data analysis, for instance on seismic events detection, signal classification, and data visualization. There are two main methods for implementing these techniques: supervised and unsupervised learning. The former is mainly used when labeled data, based on expert knowledge, is available. This approach has been used in seismology to discriminate different events and to automatically detect seismic phases (Joswig, 1990; Bai and Kennett, 2000; Ohrnberger, 2001; Riggelsen et al., 2007). The latter, unsupervised learning, allows us to cluster input data in classes based on their statistical properties by giving a probabilistic model of the data when no supervision or reward is given in the classification algorithm, allowing data to “speak by itself.” In this approach, self-organizing maps have been used for the discovery, imaging, and interpretation of temporal patterns in seismic array recordings (Kohler et al., 2009; Kohler et al., 2010).

¹Universidad Industrial de Santander.

²Ecopetrol S.A., Instituto Colombiano del Petróleo.

<http://dx.doi.org/10.1190/tle36030239.1>

In this work, we build a robust attribute model to detect and classify surface waves based on differences in seismic attributes with wave mode propagation. The practical expectations of our method are twofold: to detect the surface-wave zones by separating them from the rest of the information and to classify these surface waves into subgroups with similar behavior within the surface-wave cone zone.

To assess the performance of this surface-wave detection and classification methodology, we apply it to three different real 2D-3C data sets acquired in Colombia that exhibit a markedly differentiated behavior within the surface-wave zone. Pattern recognition was performed using the unsupervised clustering technique k -means.

***k*-means clustering algorithm**

k -means is the most popular clustering algorithm employed to partition a data set of n points into k groups so that each of the n observations belongs to the cluster with the nearest mean. Its advantage is that it is used when no a priori knowledge, such as expert classification of the data, is available. That is why it is called an unsupervised learning technique. In this method, when any information is given about where each of the data points should be placed within the partition, they are clustered according to some notion of similarity presented in the set of attributes provided to the algorithm.

The algorithm starts with the assumption that the number of clusters, k , for the database (Figure 2a) is known. When this is

not true, it is possible to use a wrapper search to find the best value of k ; however, other approaches have been proposed in literature to find the optimal number of clusters (Honarkhah and Caers, 2010). Then, k initial cluster points, known as *seeds*, are randomly chosen within the space of attributes to be the centroids of the clusters, as shown in Figure 2b. Then, each data point is grouped to the nearest centroid. After assigning all the points to their corresponding nearest centroids, the first iteration of clusters of Figure 2c is obtained.

For each iteration, the mean of each of the k clusters is recomputed, and hence the centroids are relocated (Figure 2d), changing the distribution of the data points within each cluster, as shown in Figure 2e. This procedure continues iteratively until no changes in the objective function are evident, as illustrated from Figures 2f to 2g. The objective function comes down to minimize the sum of distance functions of each point in the cluster to its centroid, given in the optimization problem 1. In summary, the search of these centroids aims to minimize the within distances while maximizing the between-cluster distances.

$$J = \sum_{j=1}^k \sum_{i=1}^n \|x_i^j - c_j\|, \quad (1)$$

where J is the objective function to be minimized, x_i^j is an attribute vector corresponding to the i th observation of the j th

Table 1. Seismic attributes computed using different attribute extraction methods in seismic data. V: vertical component, R: radial component, and T: transverse component.

Attribute extraction method	No.	Seismic attributes
Instantaneous complex trace (Morozov and Smithson, 1996)	1–3. 4–6. 7–9. 10–12. 13–15. 16–18. 19–21.	Instantaneous amplitude (V, R, T) Instantaneous phase (V, R, T) Instantaneous frequency (V, R, T) Instantaneous reciprocal ellipticity (V-R, V-T, R-T) Instantaneous signed reciprocal ellipticity (V-R, V-T, R-T) Instantaneous tilt angle (V-R, V-T, R-T) Instantaneous rise angle (V-R, V-T, R-T)
Covariance analysis (Jurkevics, 1988)	22. 23. 24. 25.	Azimuth angle Incidence angle Planarity Rectilinearity
Complex covariance analysis (Vidale, 1986)	26. 27. 28. 29.	Dip angle Strike angle Strength of polarization Degree of planar polarization
Singular value decomposition (De Franco and Musacchio, 2001; Tiapkina et al., 2012)	30. 31. 32. 33. 34.	Ground-roll detector Energy Planarity Rectilinearity along the first principal axis Rectilinearity along the second principal axis
Spectral analysis (Tiapkina et al., 2012)	35–37.	Centroid of the power spectrum (V, R, T)
Spectrum of polarization ellipsoid (Pinnegar, 2006)	38. 39. 40. 41. 42. 43. 44. 45.	Semimajor axis S-spectrum Semimajor axis S-spectrum Difference between semimajor and semiminor axis S-spectrum Total-power S-spectrum Azimuth of ascending mode S-spectrum Inclination S-spectrum Argument of maximum S-spectrum Phase S-spectrum

cluster, and c_j is the location of the centroid of the j th cluster in the attribute space.

As a final remark, it is important to note that despite this algorithm being efficient, easy to understand, and easy to implement, if the objective function J is used, it can converge to a local optimum since the global optimum is hard to find because of its complexity.

Methodology

The flowchart in Figure 3 shows step by step the methodology applied. The process in each step will be briefly explained.

- 1) *Attribute generation.* Seismic attributes were computed using six different attributes sets for a total of 45 initial attributes, all running in short time windows of 3C seismic data. Table 1 shows the seismic attributes computed for each trace.

2) *Attribute selection.* The objective of this step is threefold: improving the prediction performance, providing faster and more cost-effective predictors, and providing a better understanding of the underlying process by reducing the complexity of the model. A relevancy filter was implemented to compare the correlation between the attributes. Attributes were sorted in ascending order, and those whose correlation was greater than 0.95 were removed from the data set (see Figure 5a). A wrapper forward method was the second attribute-selection algorithm. This method considers selection as a search problem in which different combinations of seismic attributes are evaluated and compared to a human classification based on a cost function. The cost function used was the *accuracy* of classification. The k -means algorithm was used to evaluate the cost function. The search process starts by identifying the couple of attributes giving the

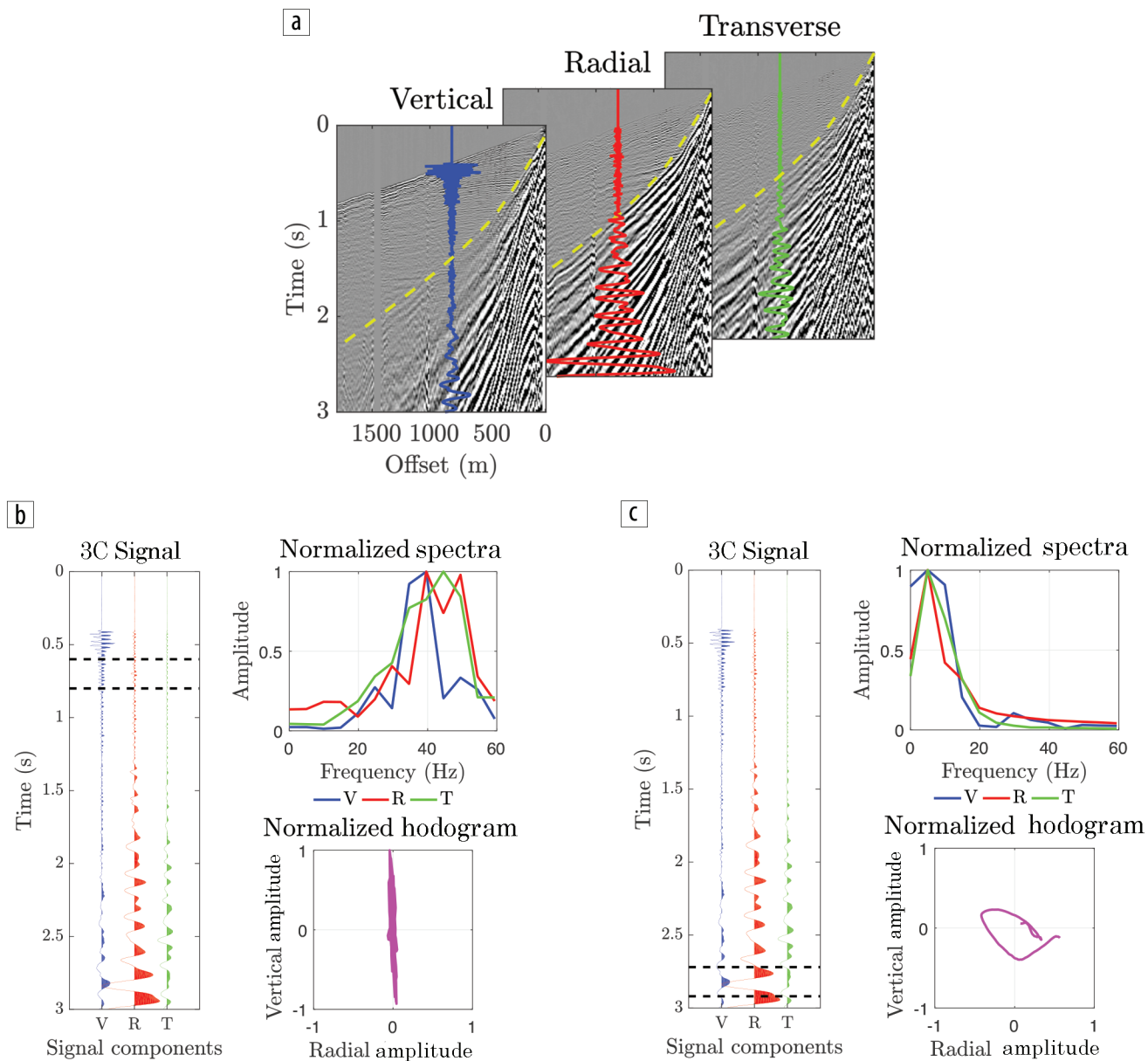


Figure 1. (a) Vertical, radial, and transverse components of the 3C seismic show gather. Comparison between (b) body-wave and (c) surface-wave behavior by means of the normalized spectra and hodograms obtained for each sliding time window.

highest accuracy classification, and each new attribute is added iteratively only if it enhances the accuracy given by the previous group. In short, this works as a recursive attribute addition algorithm.

- 3) *Classification.* In its simplest definition, classification is the procedure of deciding to which cluster an observation should be assigned based on a notion of similarity; to do so, we use the unsupervised pattern-recognition technique k -means, as explained previously.

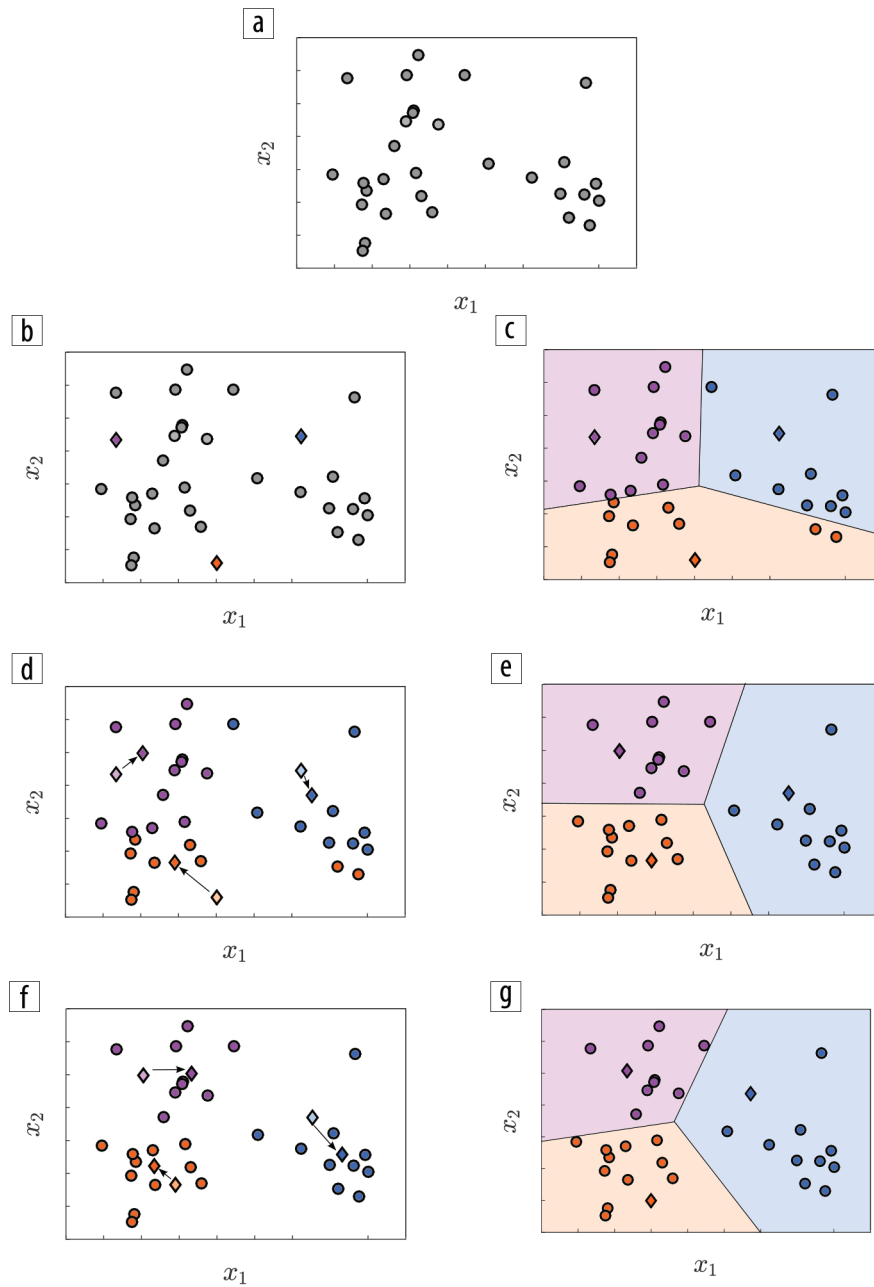


Figure 2. Clustering by k -means. In this example three classes are determined. (a) Set of datapoints. (b) The k seeds are randomly chosen within the space vector, and (c) each data point is matched to the closest centroid. (d) The means are recomputed and the centroids relocated, and (e) the distribution of the data points within each cluster is changed. (f) This process is repeated until no changes in the objective function are evident, and (g) the final classification is obtained.

Results

The detection and classification of surface waves were performed in three types of real data, each one showing well-differentiated behavior within the surface-waves zone. The first data set corresponds to a 2D-3C acquisition using a relatively low-frequency source (close to the frequencies commonly used for oil prospecting). The second and third data set is a 2D-3C acquisition using a relatively high-frequency source. Table 2 shows the acquisition parameters for each data set.

Field data example 1

Figure 4 shows the vertical, radial, and transverse components from field data 1. The attribute selection was performed following the methodology presented in the previous section. The relevancy filter made it possible to reduce the number of attributes from the 45 initials to 35 based on their correlation matrix (Figure 5a). Meanwhile, the wrapper forward method using k -means and human-labeled data made it possible to reduce the number

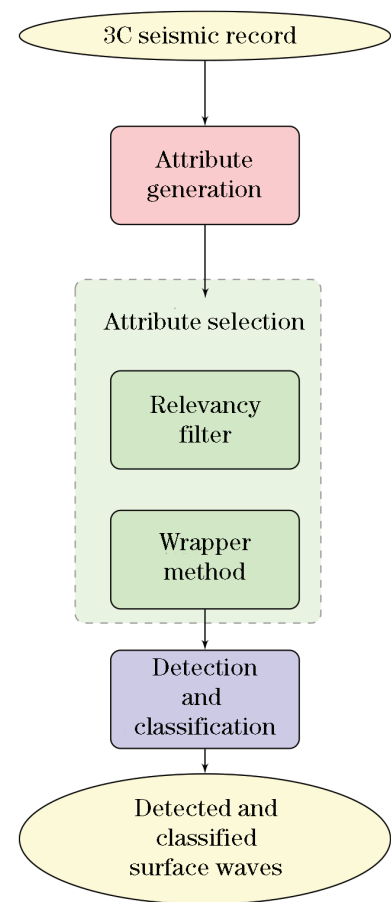


Figure 3. Flowchart showing the methodology carried out along this research.

of significant attributes to 12, based on accuracy of classification as the cost function (Figure 5b).

Figure 6a shows the areas manually labeled from the seismic record shown in Figure 4. A crossplot data of these label areas are shown in Figure 6b. Surface-wave detection was done using k -means with $k = 2$. Figure 6c and Figure 6d show the result of the detection with its corresponding scatter data.

We decided to separate the surface waves detected into two subgroups using k -means inside the surface-wave cone. Figure 6e and Figure 6f show the result of the classification and the respective scatter data. The innermost area is similar to the area labeled like surface waves in Figure 6a. Finally, we decided to separate the surface waves detected into three groups using k -means inside the surface-wave cone. The results are shown in Figure 6g. We interpret the innermost area as superficial energy limited by Rayleigh wave because of its velocity. Moreover, from scatter data in Figure 6h, it is clear that the semimajor axis S spectrum in the innermost area is higher than in other areas.

Field data example 2

The shot gathers of the second type of data are shown in Figure 7. In this data set, a more homogeneous behavior within the surface-wave zone is evident. After following the flowchart given in Figure 3, the correlation matrix illustrated in Figure 8a is obtained and, as a result, nine attributes were removed. The accuracy of the surface-wave detection as a function of the number of the remaining 36 attributes is shown in Figure 8b. From this figure, we may conclude that only three attributes are necessary to achieve the best result.

The figure showing the labeled zones and the scatterplot of two attributes are shown in Figures 9a and 9b, respectively. In Figure 9c the surface-wave zones are detected by using k -means with $k = 2$, and Figure 9d shows the correspondent crossplot with two attributes. As surface waves in this data set present a homogeneous behavior, the classification was not performed by clustering in the detected surface waves but in the entire data set. Then, the classification of these surface waves is performed by using k -means with $k = 2$, as shown in Figure 9e. The algorithm makes it possible to identify a second zone of surface waves. The green area may correspond to the backscattered surface waves. The corresponding crossplot with the same two attributes is shown in Figure 9f.

Field data example 3

The shot gathers of the third data set are shown in Figure 10. In this kind of data, a very inhomogeneous behavior within the surface-wave zone is present. In this case, the two steps of the flowchart in Figure 3 were not performed. Instead, we took the same attributes selected in the previous case to detect the surface waves. Figures 11a and 11b depict the results of the detection by using k -means with $k = 2$, and Figures 11c and 11d depict the results of the detection by using k -means with $k = 3$.

Discussion: Clustering of seismic attributes

Seismic attributes for surface-wave detection allow one to numerically differentiate surface waves from reflections. In some cases, this differentiation is performed by determining thresholds

Table 2. Information about seismic acquisitions for the three sets of real data used in this work.

Information	Field data 1	Field data 2	Field data 3
Source type	Explosive gel	Explosive gel/caps	Explosive gel/caps
Load size	1800 g	150 g	150 g
Source depth	10 m	7.5 m	7.5 m
Receiver interval	10 m	5 m	5 m
Maximum offset	1800 m	100 m	300 m
Sampling rate	2 ms	0.5 ms	0.5 ms
Data bandwidth	3–120 Hz	5–450 Hz	5–500 Hz

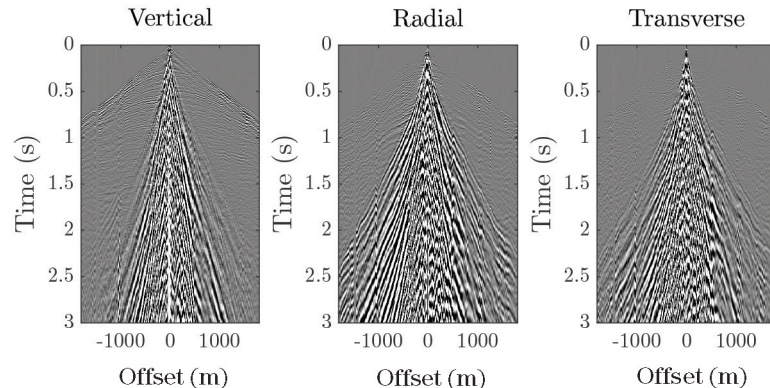


Figure 4. Vertical, radial, and transverse components of the first data set.

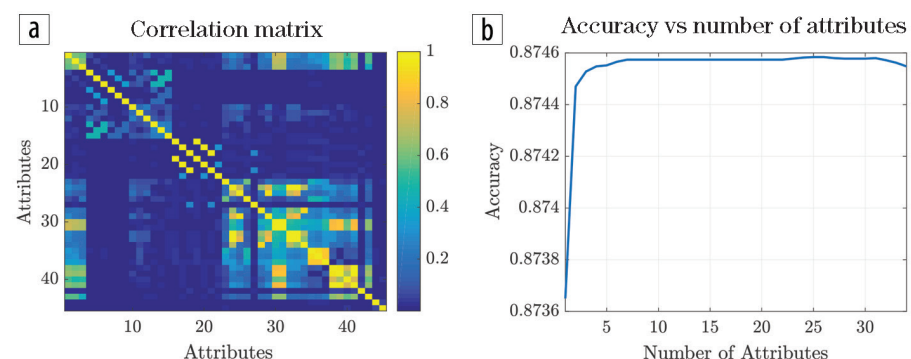


Figure 5. (a) Correlation matrix for the relevancy filter using the original 45 seismic attributes in the first data set. Ten attributes showed high cross correlation, and they were removed. (b) Classification accuracy using k -means classifier on labeled data for the remaining 35 seismic attributes versus number of attributes.

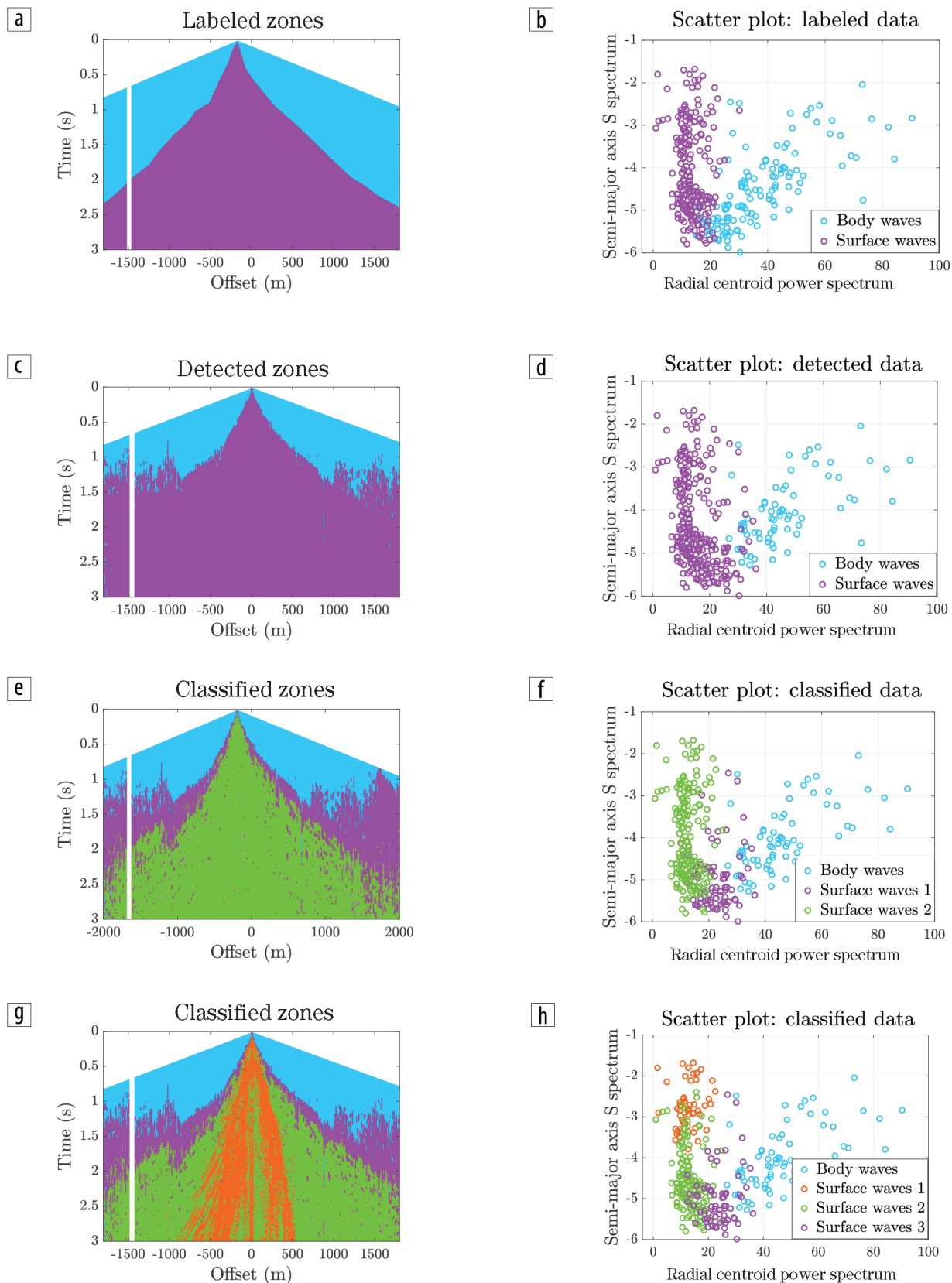


Figure 6. Results of surface-wave detection and classification for data set 1. (a) Areas from the seismic record labeled by experts. (b) Scatter data of labeled areas. (c) Areas detected by k -means with $k = 2$. (d) Scatter data of detected areas by k -means with $k = 2$. (e) Areas classified by k -means with $k = 2$ within the cone, allow to identify two different wave modes within the surface waves area; see Sánchez et al. (2016) for further details. (f) Scatter data of classified areas by k -means with $k = 2$ inside the cone. (g) Areas classified by k -means with $k = 3$ within the cone, allow to identify three different wave modes within the surface waves area. (h) Scatter data of classified areas by k -means with $k = 3$ inside the surface waves cone.

in a heuristic way. Then, results are biased by human judgment; to mitigate possible errors with these methods, minimizing the classification cost function is a solution.

From the previous results, it is clear that not all attributes are created equally. In our field data example, some attributes had high correlation, and it was a necessary stage of attribute selection to have an optimal set of attributes. These seismic attributes can be clustered in families in which each family can describe a behavioral pattern in particular.

Based on the results obtained in the detection of the surface-wave cone of Figure 1, it is possible to conclude that in spite of the fact that the automatic detection differs from the manually labeled data in the adjacent zones just above the cone, in general the attributes were able to successfully describe the surface-wave behavior to ease its automatic distinction from the body waves. When the difference area (violet color) is examined, corresponds to a zone with different characteristics from the body waves and the surface waves, possibly is related to S-wave refractions and guided waves. A further k -means classification separates a green and orange area. The green area may be interpreted as higher modes of Rayleigh waves, while the orange is possibly related to scattering and reverberations.

The results in the field data example 2 are quite different from what was obtained in the first example. There is no differentiated inner surface-wave cone but only a strong outer-limit band (associated with pure Rayleigh waves). When performing the attribute selection and classification, unlike in the previous case, only this strong-amplitude outer band is clearly identified by the algorithm. The absence of inner energy in the surface-wave cone can be explained by two characteristics in the seismic source: (1) it is a small source (explosive mass 150 g) of low energy and high frequency so that reverberations and scattering resulting of medium heterogeneities are reduced (the relation of wavelength and near-surface thickness and heterogeneity size has changed); and (2) unlike the clearly cylindrical 1800 g source of the first field data (explosive dimensions were 320 cm height and 15 cm hole diameter), the 150 g source was closer to a spherical source (15 cm \times 15 cm), which is more symmetrical and less prone to generate shear energy. It is interesting to note that a possible Rayleigh wave backscattering linear event is partially identified by the algorithm (green color linear event with negative slope starting at 0.6 s and offset +50 m in Figure 9e).

The field data example 3 (Figure 10) was performed in a zone with rough topography and rapidly varying near-surface

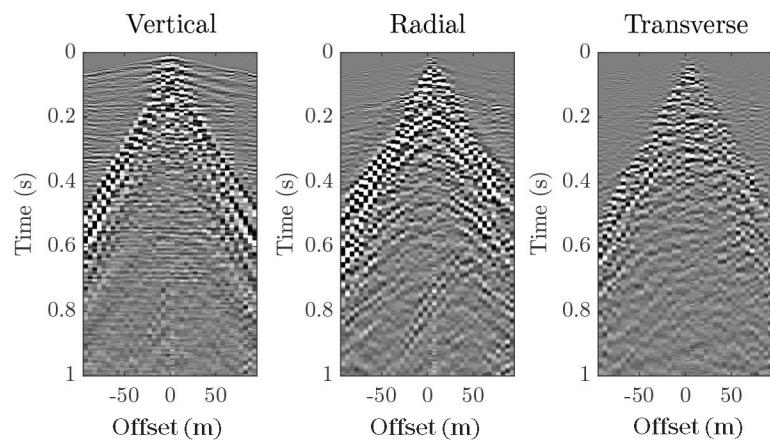


Figure 7. Vertical, radial, and transverse components of the second data set.

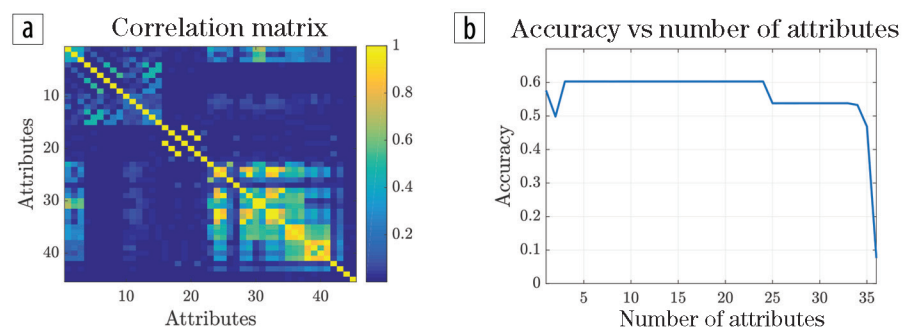


Figure 8. (a) Correlation matrix for the relevancy filter using the original 45 seismic attributes in the second data set. Nine attributes showed high cross correlation, and they were removed. (b) Accuracy of classification by using k -means classification on labeled data for the remaining 36 seismic attributes versus number of attributes.

properties (thickness and velocity). In this case, a human interpretation is challenging due to the complexity in the surface-wave characteristics. Here, pattern-recognition techniques show at their best. We used the attributes chosen in a flat topography area (field data example 2), where they can be guided during the relevance filter stage and then applied in the more complex data example 3. Surface-wave limit is clearly identified (green color Figure 11c). A band of high amplitude is identified (violet color) that could correspond to a localized scattering caused by the topographic and thickness variations in this rough topography area.

Two disadvantages of the k -means algorithm are: (1) the location of the seeds needed to start the iterative process and the optimal number of clusters k that best clusters the data set must be determined for each problem, and (2) the selection of the seeds' position is done randomly, which can affect the repeatability of the clustering. As a future work, it is highly recommended to find the optimum values of the k clusters and try different methods for seeding selection.

Our selection of seismic attributes has been somehow biased toward single-station multicomponent attributes. A suggested continuation of this work implies the use of multistation seismic attributes to take into account other attributes like the velocity (slope) of movement of the particles (Bear et al., 1999; De Meersman et al., 2006).

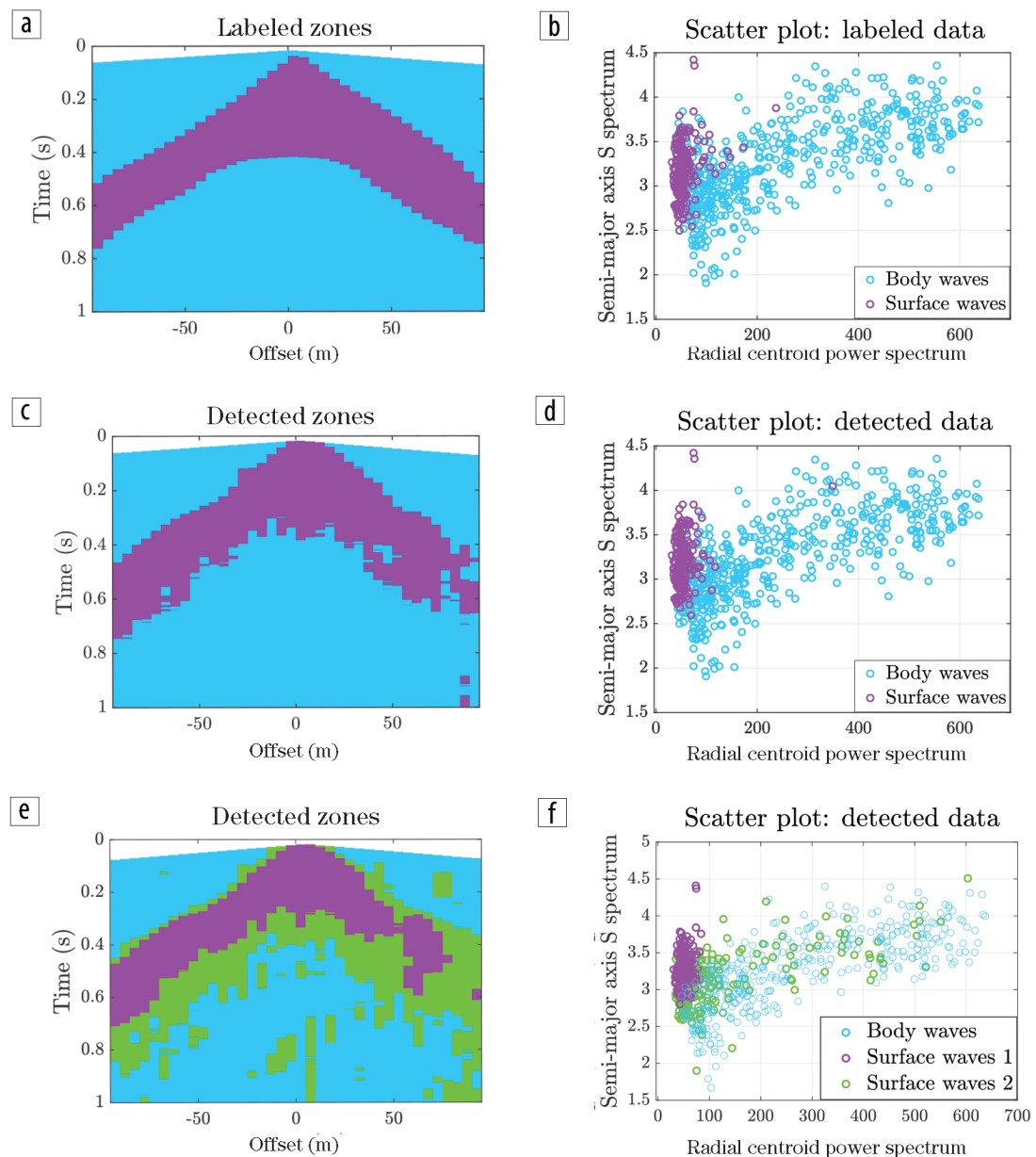


Figure 9. Results of surface-wave detection and classification for data set 2. (a) Areas from the seismic record labeled by experts. (b) Scatter data of labeled areas. (c) Areas detected by k -means with $k = 2$. (d) Scatter data of detected areas by k -means with $k = 2$. (e) Areas classified by k -means with $k = 3$. Two different wave modes of surface waves were identified. (f) Scatter data of detected areas by k -means with $k = 3$.

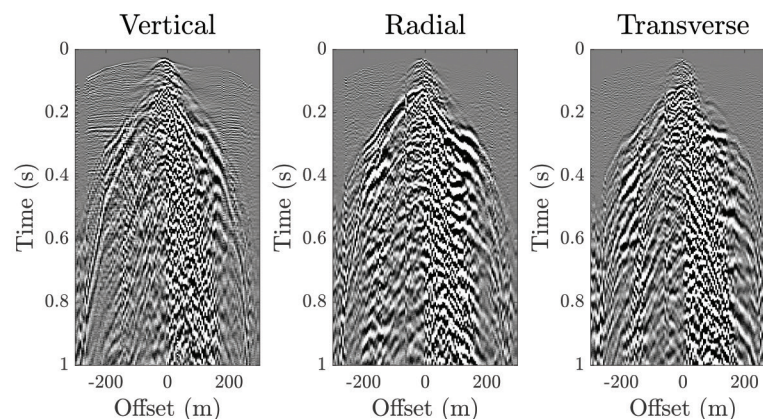


Figure 10. Vertical, radial, and transverse components of the third data set.

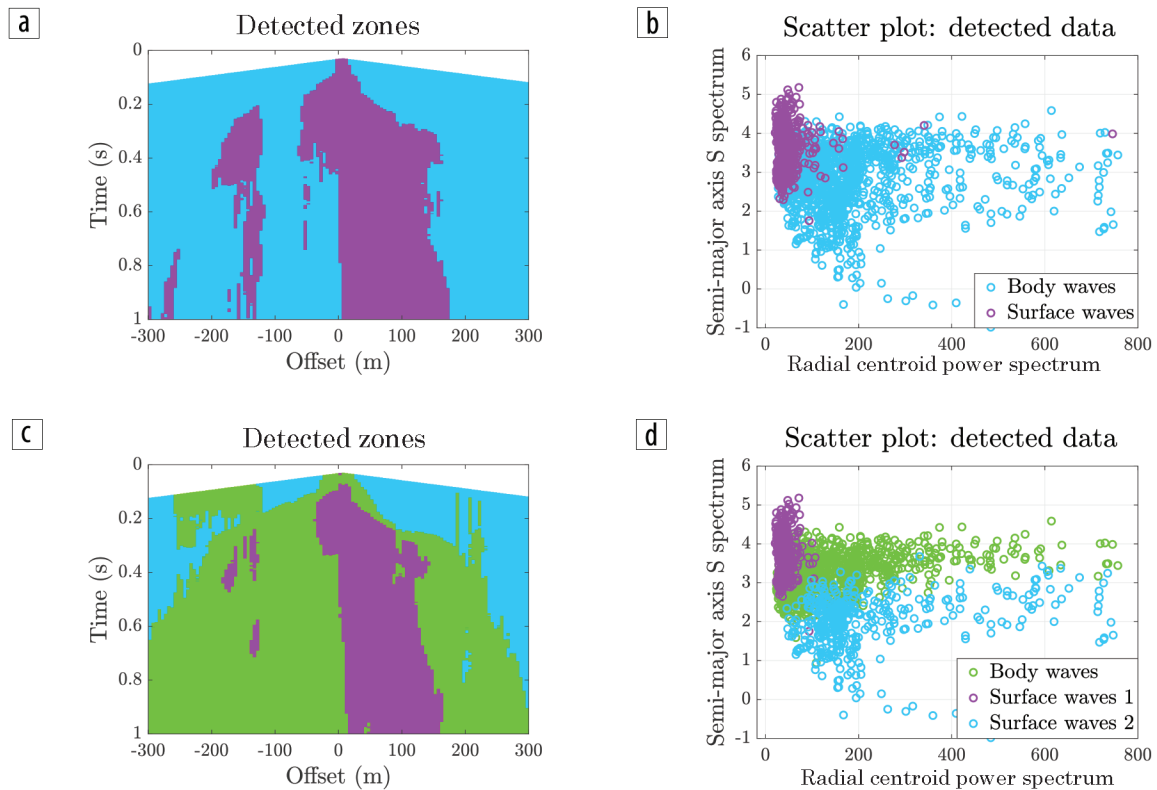


Figure 11. Results of surface-wave detection and classification for data set 3. (a) Areas classified by k -means with $k = 2$. (b) Scatter data of detected areas with $k = 2$. (c) Areas classified by k -means with $k = 3$. (d) Scatter data of detected areas $k = 3$.

Further work will explore the applications of this technique in processing (filtering) and inversion of surface waves. Automatic classification by pattern recognition could potentially improve the processing of seismic data by the design of adaptive filters for ground-roll attenuation, tailored to each region by its characteristic attributes. That honors the real complexity of surface waves and could potentially optimize the separation of reflection energy from surface waves.

Additionally, the current practice of surface-wave inversion tries to indiscriminately fit all the modes present in the surface-wave cone, even if they correspond to different propagation phenomena. Thus, attributes classification could be used as an extra step before inversion, in a sort of cascade system, that allows to separate the different wave modes (pure Rayleigh, higher modes, scattering, etc.) identified within the surface-wave cone, so that a refined and better fitted inverse modeling can be done. **TLF**

Acknowledgments

This work was carried on the framework of the Agreement “Acta No. 4 del Convenio de Cooperación Tecnológica 5211794” between Universidad Industrial de Santander and Ecopetrol S.A.- Instituto Colombiano del Petróleo. We are grateful to Saúl Guevara and Carlos Niño for the fruitful discussions about the use of attributes in surface-wave classification.

Corresponding author: ivanjavier240@gmail.com

References

- Bai, C. Y., and B. L. N. Kennett, 2000, Automatic phase-detection and identification by full use of a single three-component broadband seismogram: *Bulletin of the Seismological Society of America*, **90**, no. 1, 187–198, <http://dx.doi.org/10.1785/0119990070>.
- Bear, L. K., G. L. Pavlis, and G. H. Bokelmann, 1999, Multi-wavelet analysis of three-component seismic arrays: Application to measure effective anisotropy at Pinon Flats, California: *Bulletin of the Seismological Society of America*, **89**, no. 3, 693–705.
- De Franco, R., and G. Musacchio, 2001, Polarization filter with singular value decomposition: *Geophysics*, **66**, no. 3, 932–938, <http://dx.doi.org/10.1190/1.1444983>.
- De Meersman, K., M. Van der Baan, and J. M. Kendall, 2006, Signal extraction and automated polarization analysis of multicomponent array data: *Bulletin of the Seismological Society of America*, **96**, no. 6, 2415–2430, <http://dx.doi.org/10.1785/0120050235>.
- Honarkhah, M., and J. Caers, 2010, Stochastic simulation of patterns using distance-based pattern modeling: *Mathematical Geosciences*, **42**, no. 5, 487–517, <http://dx.doi.org/10.1007/s11004-010-9276-7>.
- Joswig, M., 1990, Pattern recognition for earthquake detection: *Bulletin of the Seismological Society of America*, **80**, no. 1, 170–186.
- Jurkevics, A., 1988, Polarization analysis of three-component array data: *Bulletin of the Seismological Society of America*, **78**, no. 5, 1725–1743.
- Köhler, A., M. Ohrnberger, and F. Scherbaum, 2009, Unsupervised feature selection and general pattern discovery using self-organizing maps for gaining insights into the nature of seismic wavefields: *Computers & Geosciences*, **35**, no. 9, 1757–1767, <http://dx.doi.org/10.1016/j.cageo.2009.02.004>.

- Köhler, A., M. Ohrnberger, and F. Scherbaum, 2010, Unsupervised pattern recognition in continuous seismic wavefield records using self-organizing maps: *Geophysical Journal International*, **182**, no. 3, 1619–1630, <http://dx.doi.org/10.1111/j.1365-246X.2010.04709.x>.
- Morozov, I. B., and S. B. Smithson, 1996, Instantaneous polarization attributes and directional filtering: *Geophysics*, **61**, no. 3, 872–881, <http://dx.doi.org/10.1190/1.1444012>.
- Ohrnberger, M., 2001, Continuous automatic classification of seismic signals of volcanic origin at Mt. Merapi, Java, Indonesia: Doctoral thesis, University of Potsdam.
- Pinnegar, C. R., 2006, Polarization analysis and polarization filtering of three-component signals with the time–frequency S transform: *Geophysical Journal International*, **165**, no. 2, 596–606, <http://dx.doi.org/10.1111/j.1365-246X.2006.02937.x>.
- Riggelsen, C., M. Ohrnberger, and F. Scherbaum, 2007, Dynamic Bayesian networks for real-time classification of seismic signals, in J. N. Kok, J. Koronacki, R. L. de Mantaras, S. Matwin, D. Mladenić, A. Skowron, eds., *Knowledge Discovery in Databases: PKDD 2007*: Springer Berlin Heidelberg, 565–572, http://dx.doi.org/10.1007/978-3-540-74976-9_59.
- Sánchez, I. J., J. O. Serrano, C. A. Niño, D. A. Sierra, and W. A. Agudelo, 2016, SVD polarization filter taking into account the planarity of ground roll energy, *Ciencia: Tecnología y Futuro*, **6**, no. 3, 5–16.
- Sheriff, R. E., 2002, Encyclopedic dictionary of applied geophysics: SEG, <http://dx.doi.org/10.1190/1.9781560802969>.
- Tiapkina, O., M. Landrø, Y. Tyapkin, and B. Link, 2012, Single-station SVD-based polarization filtering of ground roll: Perfection and investigation of limitations and pitfalls: *Geophysics*, **77**, no. 2, V41–V59, <http://dx.doi.org/10.1190/geo2011-0040.1>.
- Vidale, J. E., 1986, Complex polarization analysis of particle motion: *Bulletin of the Seismological Society of America*, **76**, no. 5, 1393–1405.